JGR Space Physics

RESEARCH ARTICLE
10.1029/2020JA028010

Impact of Martian Crustal Magnetic Field on the Ion Escape

E. Dubinin[1], M. Fraenz[1], M. Pätzold[2], J. Woch[1], J. McFadden[3], K. Fan[4], Y. Wei[4], O. Tsareva[5], and L. Zelenyi[5]

[1]Max-Planck-Institute for Solar System Research, Göttingen, Germany, [2]Abteilung Planetforschung, Rheinisches Institut fuer Umweltforschung, Cologne, Germany, [3]Space Sciences Laboratory, University of California, Berkeley, CA, USA, [4]Institute of Geology and Geophysics, Key Lab of Earth and Planetary Physics, Beijing, China, [5]Institute of Space Research, Moscow, Russia

Key Points:
- Crustal magnetic field at Mars has a twofold effect on atmospheric erosion
- At lower altitudes the crustal fields form a protective shield around the ionized atmosphere
- Due to expansion of ionosphere to higher altitudes, a larger cross-section area is exposed to the solar wind that increases ion losses

Correspondence to:
E. Dubinin,
dubinin@mps.mpg.de

Citation:
Dubinin, E., Fraenz, M., Pätzold, M., Woch, J., Mcfadden, J., Fan, K., et al. (2020). Impact of Martian crustal magnetic field on the ion escape. *Journal of Geophysical Research: Space Physics*, *125*, e2020JA028010. https://doi.org/10.1029/2020JA028010

Received 17 MAR 2020
Accepted 3 SEP 2020
Accepted article online 9 SEP 2020

Abstract Based on the Mars Atmosphere and Volatile EvolutioN (MAVEN) observations, we have analyzed the role of the crustal magnetic field on ion loss driven by the direct interaction of the solar wind with the Mars ionosphere. Crustal magnetic fields significantly attenuate the ion ionospheric motions and raise the flux of returning ions. On the other hand, since the ion densities in the ionosphere with strong crustal field are significantly higher than in the ionosphere with a weak crustal magnetic field, the net escape fluxes from the ionosphere with the crustal sources remain vital. The crustal magnetic field also leads to the expansion of the ionosphere and increase of the area exposed to solar wind. As a result, fluxes from higher altitudes essentially contribute to the flow pattern in Martian tail producing an excess of ion loss rate (~15%) through the southern part of the tail. Thus, effects of inhibition and enhancement of the escape rate by the crustal magnetic field at Mars operate in competition producing a minor influence on the total ion loss.

1. Introduction

The question whether a planetary magnetic field protects its atmosphere from the solar wind erosion or, in contrast, enhances the atmospheric loss by opening channels through which energy from the solar wind is transferred and focused toward the atmosphere is widely debated (Egan et al., 2019; Gunell et al., 2018; Moore & Horwitz, 2007; Strangeway et al., 2010; Tsareva et al., 2020). Mars has no intrinsic magnetic field, and solar wind is in a direct contact with the atmosphere. On the other hand, there are rather large localized areas on Mars (Acuna et al., 1999) with strong crustal magnetization, which add important features to the interaction typical for intrinsic magnetospheres. Since the solar wind-induced escape might be a dominant process for atmosphere and water losses from Mars (Barabash et al., 2007; Brain et al., 2015; Dubinin et al., 2011; Lundin et al., 1989), the role of the crustal magnetic field in such a process becomes important. Based on Mars Global Surveyor (MGS) observations, Brain et al. (2010) have found that the crustal fields create an additional escape channel by forming flux ropes along elongated crustal field lines. Hundreds of large-scale flux ropes occurring near the strong crustal fields have been detected at an altitude of 400 km (Brain et al., 2010). Their frequent ejection to the tail can carry away significant amounts of particles from the atmosphere. Flux ropes with sizes comparable to half a planetary radius initiated by reconnection were observed in simulations too (Harnett, 2009).

Analyzing the Mars Express measurements made by the ASPERA-3 instrument, Lundin et al. (2011) have observed higher escape fluxes of the low-energy ions ($E \leq 200$ eV) at the dayside over the regions with strong crustal magnetization. On the other hand, these authors did not find evidence for a further ion transport tailward, suggesting a cycling of ions within the minimagnetospheres generated by the small-scale planetary crustal fields. Observations made by Nilsson et al. (2011) have confirmed that the low-altitude ion fluxes are higher in the Southern Hemisphere, where the strongest crustal magnetic sources are located, while the net escape through the tail is lower (~75%) as compared to the Northern Hemisphere, implying a shielding effect of the crustal magnetic field. Using the observations by Mars Express obtained over 8 years, Ramstad et al. (2016) have found that the orientation of the crustal field sources related to the Mars rotation modulates the ion loss rate. The minimum/maximum escape rates were observed when the strongest crustal fields occurred at the dayside (solar zenith angles SZA ~20–60°) and near the terminator (SZA ~60–80°),

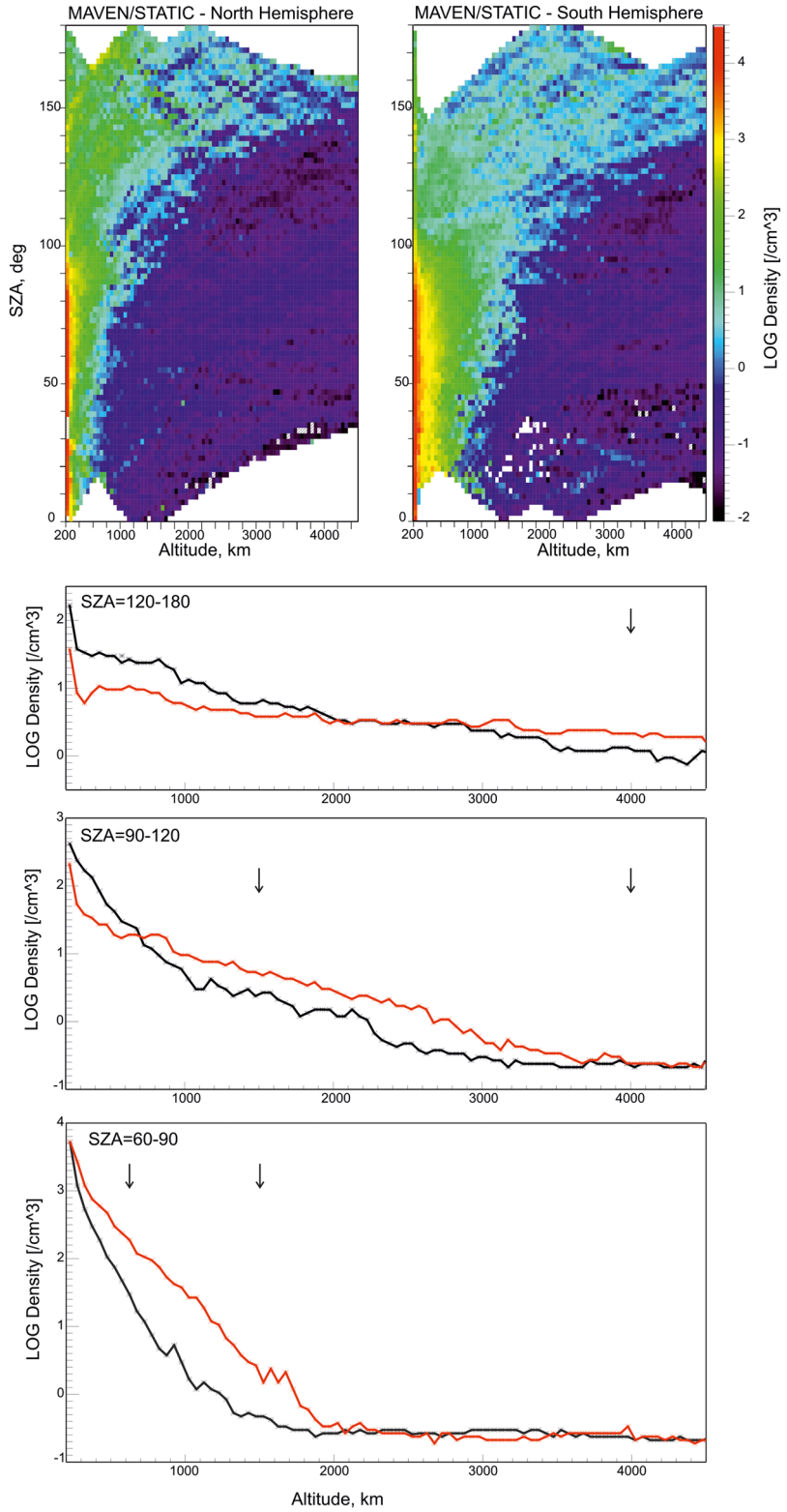

Figure 1. Maps of the median values of the oxygen ($O^+ + O_2^+$) ion number density in the northern and the southern quadrants with the weak and strong crustal magnetic field, respectively. Lower panels show the altitude profiles of the ion number density in several ranges of solar zenith angles. Black (red) curves correspond to the northern (southern) quadrants, respectively.

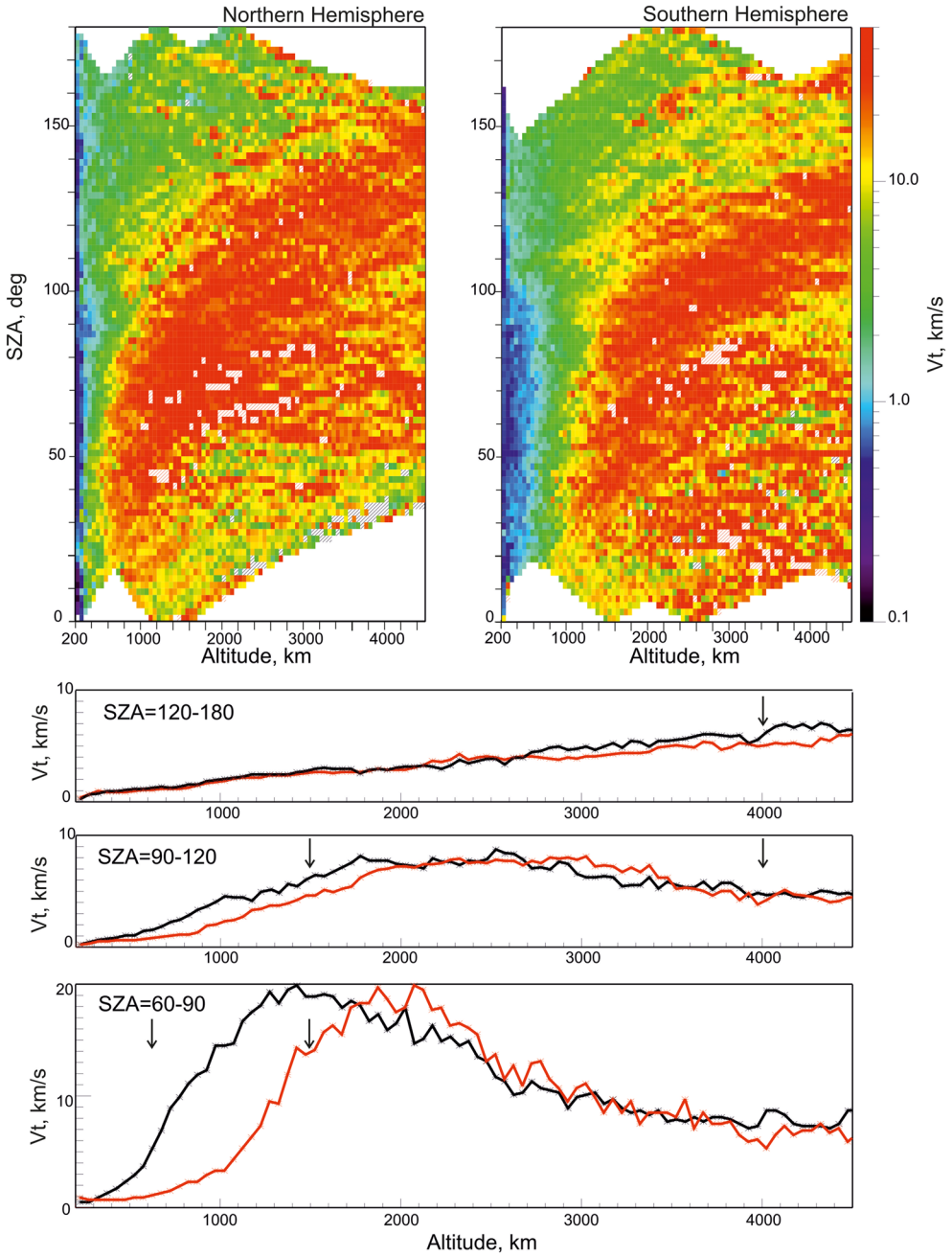

Figure 2. Maps of the median values of the density averaged oxygen ion speed in the northern and the southern quadrants with the weak and strong crustal magnetic field, respectively. Lower panels show the altitude profiles of the ion velocity in several ranges of solar zenith angles (black [red] in the northern [southern] quadrants, respectively).

respectively. On the other hand, Ramstad et al. (2016) have found no statistically significant difference in the escape rates from the Northern and the Southern Hemispheres. Analyzing the MAVEN data, Fan et al. (2019) have shown that fluxes of oxygen ions with $E \geq 30$ eV observed above the regions with strong crustal magnetic field are reduced as compared to fluxes in the regions with a weak crustal field.

Effects of the crustal magnetic field on escape rates were also widely investigated by simulations. Ma et al. (2002) have found a ~30% reduction of escape rate when the crustal magnetic field was included to the MHD model. Brecht and Ledvina (2014), based on hybrid simulations, have shown a much stronger reduction of the overall escape rate by suppressing ion motions within the ionosphere with crustal sources. Ma et al.

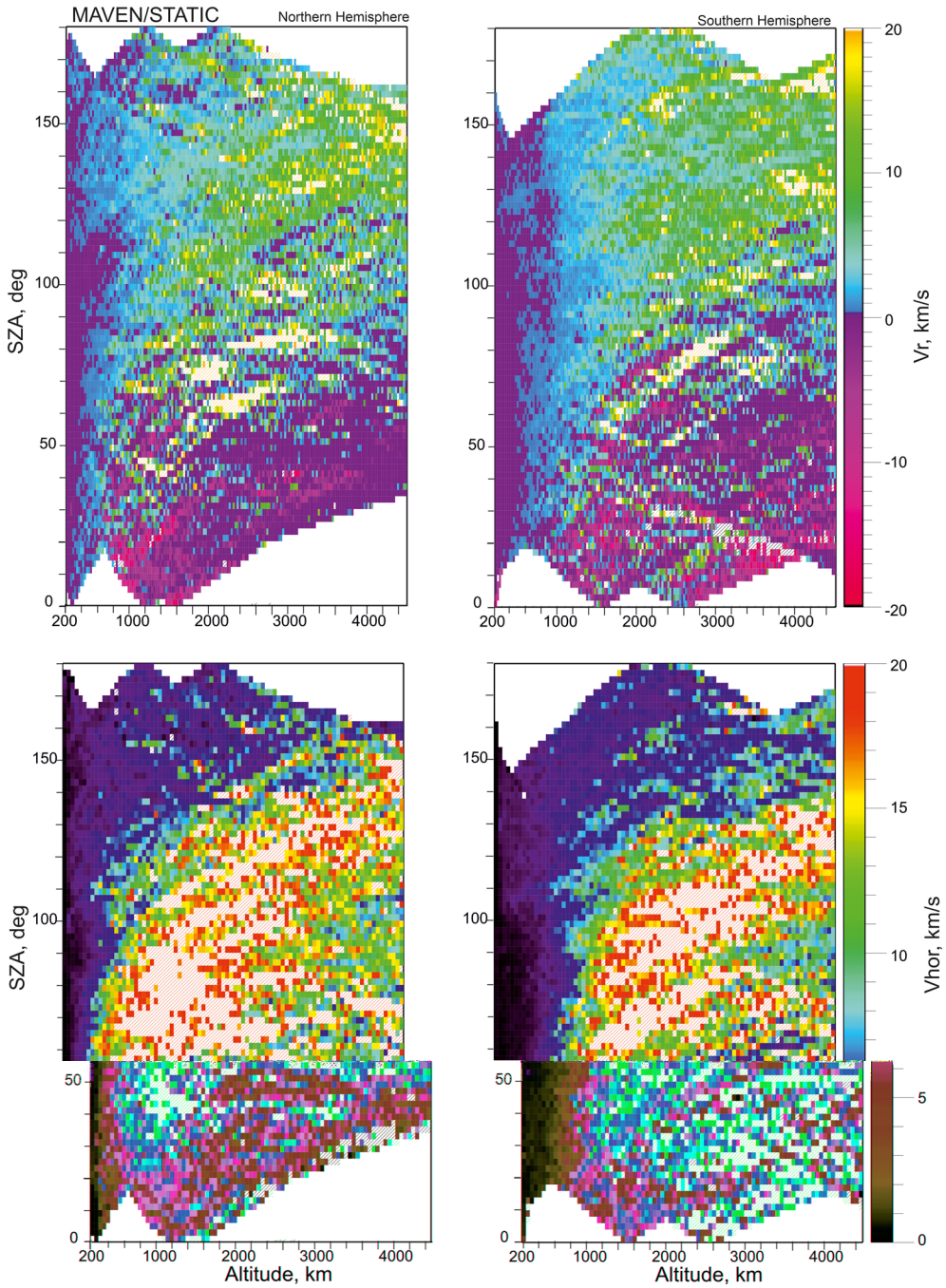

Figure 3. Maps of the median values of the radial (upper panels) and horizontal (lower panels) components of the ion velocities in the northern (left panels) and the southern (right panels) quadrants with the weak and strong crustal magnetic field, respectively. In red shaded bins the velocity is above 20 km/s.

(2014) applied a time-dependent MHD model to study how the varying location of the crustal magnetic fields due to the Mars rotation affects the pattern of ion loss. They have found that the ion escape rates slowly vary with rotation, generally anticorrelating with the strength of subsolar magnetic crustal sources. Fang et al. (2015) have also observed in MHD simulations that the rotating crustal fields generate time variations in escaping ion fluxes—~20% and ~50% during the entire rotation period for O^+ and for O_2^+, respectively. On the other hand, Fang et al. (2015) found that the crustal field position regulates the cross-section area available for escaping fluxes with a strong positive correlation between this area and ion losses. Sakai et al. (2018)

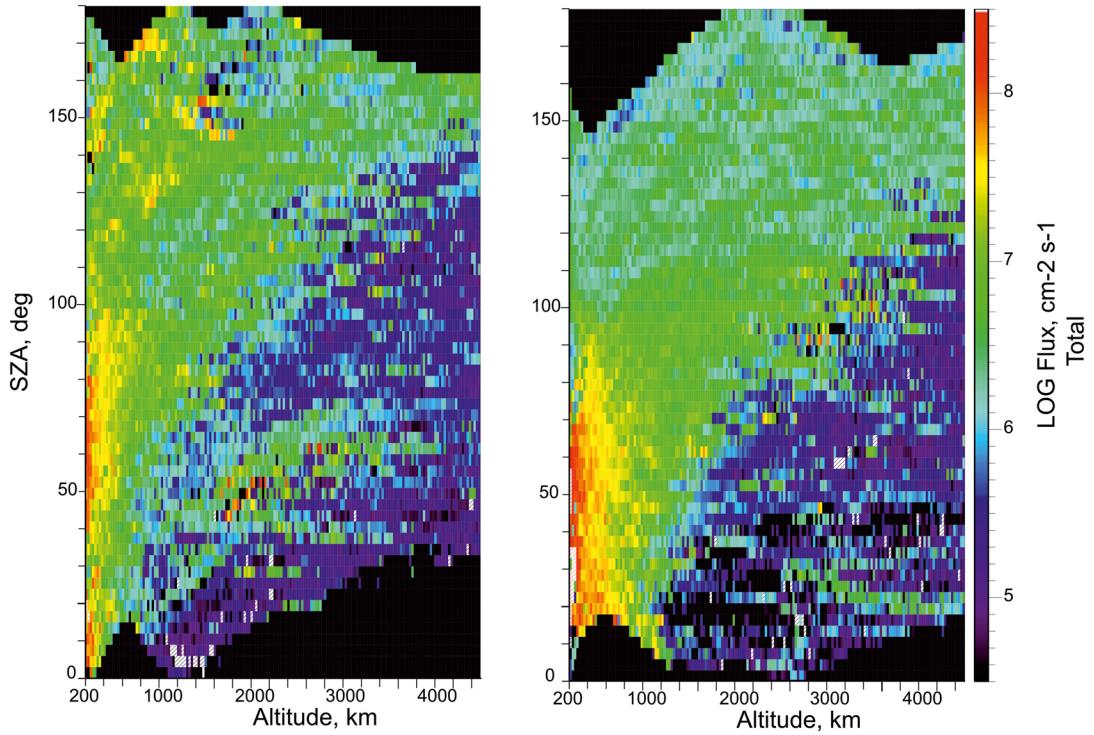

Figure 4. Maps of the median values of the total flux of oxygen ions in the northern (left panel) and the southern (right panel) quadrants with the weak and strong crustal magnetic field, respectively.

have found in their MHD model an increased escape rate for a weakly magnetized Mars (100 nT) compared to an unmagnetized case.

The ionosphere shielding by the crustal magnetic field at Mars can be also seen from the observed asymmetry of the ionosphere. The topside ionosphere above the areas with strong crustal magnetic field in the dayside Southern Hemisphere is significantly denser and expands to higher altitudes as compared to the ionosphere above the northern nonmagnetized lowlands (Andrews et al., 2013; Dubinin, Fraenz, et al., 2019; Dubinin et al., 2012). The measurements of the total electron content (TEC) in the Martian ionosphere also show a distinct trend of higher TEC in the ionosphere with high strength of the crustal field (Dubinin et al., 2016). On the other hand, the observations in the Martian tail do not reveal a clear asymmetry in ion fluxes between the Northern and Southern Hemispheres (Lundin et al., 2011; Ramstad et al., 2016).

In this paper we try to solve this paradox. In our analysis we use the observations made by the MAVEN spacecraft. The MAVEN spacecraft arrived at Mars in 2014 to study the processes in the upper atmosphere/ionosphere and its interaction with the solar wind (Jakosky et al., 2015). MAVEN was inserted into an elliptical orbit with periapsis and apoapsis of 150 and 6,200 km, respectively, and with a period of 4.5 hr. The Supra-Thermal And Thermal Ion Composition (STATIC) instrument mounted on the MAVEN spacecraft is used to study the escape of planetary ions. It measures energy spectra of ion fluxes in the range of 0.1 eV to 30 keV and the ion composition (McFadden et al., 2015). The instrument consists of a toroidal top hat electrostatic spectrometer with an electrostatic deflector at the entrance providing 360° × 90° field of view combined with a time-of-flight velocity analyzer resolving the major ion species H^+, He^{++}, He^+, O^+, O_2^+, and CO_2^+. In this paper we focus on analysis of fluxes of oxygen ions measured from November 2014 till May 2018. We also used the magnetic field data from two independent triaxial fluxgate magnetometers (MAG) (Connerney et al., 2015). It is worth noting that the measurements of the low-energy ion component (≤50 eV) on Mars Express were carried out by the ASPERA-3 sensor with a very narrow elevation field of view (~6°) and without the elevation scanning which might affect the observed escape rates (Fraenz et al., 2010, 2015). The ion observations by MAVEN have provided us a better determination of the 3-D distribution of ions in the low energy range that is important since the low-energy ($E \leq 30$ eV) component primarily contributes to

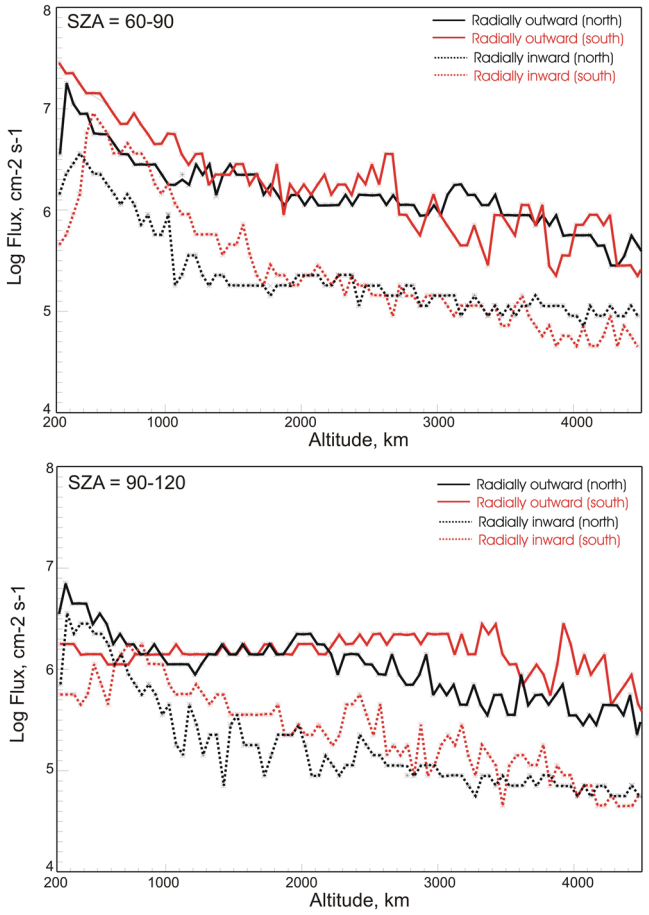

Figure 5. Median values of the ion fluxes in the radial direction in the northern (black curves) and the southern (red curves) quadrants at SZA = 60–90° and 90–120°. Solid and dotted lines show the total fluxes with outward and inward to the planet components of the ion speed, respectively.

the ion loss rate through the Martian tail (Dubinin et al., 2017; Fraenz et al., 2010, 2015; Ramstad et al., 2017).

2. Observations

Figure 1 compares the density maps of oxygen ions ($n_{tot} = n_{O^+} + n_{O_2^+}$) plotted as a function of altitude and solar zenith angle for two quadrants in the Northern and the Southern Hemisphere, respectively. The northern (southern) quadrant comprises the measurements made in the range of the areographic coordinates: Latitude = 10–70°, Longitude = 160–240° (Latitude = −10° to −70°, Longitude = 160–240°), respectively, which correspond to the regions with strong and weak crustal fields (see Figure 2c in Dubinin, Fraenz, et al., 2019). Note that latitudes >|70°| were not sampled by the MAVEN spacecraft. Here and further in the paper we used a size of bin 50 km × 2°. Lower panels show the density profiles at different SZA (red = south; black = north). Arrows mark the nominal positions of the induced magnetosphere boundary (Dubinin et al., 2006) at the corresponding solar zenith angles. We observe a distinct asymmetry between two hemispheres. At the dayside, the ionosphere above the southern lowland expands to higher altitudes. At SZA = 60–90° the difference in the density increases with height reaching a factor of ~20 at $h \sim 1{,}000$ km. At the nightside, near the terminator (SZA = 90–120°), at $h \leq 700$ km the ionosphere without strong crustal sources is denser but at higher altitudes, the density in the southern quadrant becomes higher. At SZA = 120–180° the ionosphere in the Southern Hemisphere filled by strong crustal magnetic field sources occurs more depleted as compared to the Northern Hemisphere up to 2,000–3,000 km.

Figure 2 compares similar maps of the total value of the speed $V_{tot} = (n_{O^+} V_{O^+} + n_{O_2^+} V_{O_2^+})/(n_{O^+} + n_{O_2^+})$, where the total velocity of ions species is $V_i = (V_{ix}^2 + V_{iy}^2 + V_{iz}^2)^{1/2}$ ($i = O^+, O_2^+$). Over the region with strong crustal magnetic field, the speeds of oxygen ions are significantly reduced as compared to the ion speeds in the ionosphere in the Northern Hemisphere (see the lower panels). For example, at SZA = 60–90°, the ion bulk speed of O^+ and O_{2+} ions in the southern ionosphere is reduced by factor of 5. Near the terminator, at the nightsise (SZA = 90–120°), the velocity suppression becomes smaller (factor of 1.5–2). At SZA = 120–180° we do not observe an effect of inhibition by the crustal field.

Figure 3 shows maps of the radial (V_r) and horizontal (V_{hor}) components of the ion mass velocity in the northern and southern quadrants. Positive (negative) sign of the radial component corresponds to the outward (inward) direction from the planet. A reduction of the velocities in the area with the strong crustal field is notably exposed in the horizontal component. Another important feature is that horizontal motions dominate in escape process in both hemispheres and therefore might be used to characterize the main ion loss rate through the tail.

Comparing maps of the total fluxes ($n_{tot} V_{tot}$) of oxygen ions measured in the northern and southern quadrants (Figure 4), we find that fluxes in the Southern Hemisphere dominate and cover a larger area. This result should be not surprising because the differences in ion speeds (Figures 2 and 3) are much less than the differences in the ion densities (Figure 1) and the effect of the density enhancement overcomes the velocity reduction. However, one could not here draw a simple conclusion that existence of the crustal fields enhances the ion losses. We have to take into consideration the flux direction. Indeed, the picture occurs more complicated.

Figure 5 compares, for example, the median values of the ion fluxes in the radial direction in the both quadrants at SZA = 60–90° and 90–120°. Black and red curves correspond to the measurements in the northern and the southern quadrants, respectively. Solid and dotted lines show the total fluxes with outward and inward to the planet components of the ion speed, respectively. At SZA = 60–90° and $h \leq$ ~1,000 km, fluxes in the Southern Hemisphere are higher than in the Northern Hemisphere. At SZA = 90–120° and $h \leq$ ~800 km,

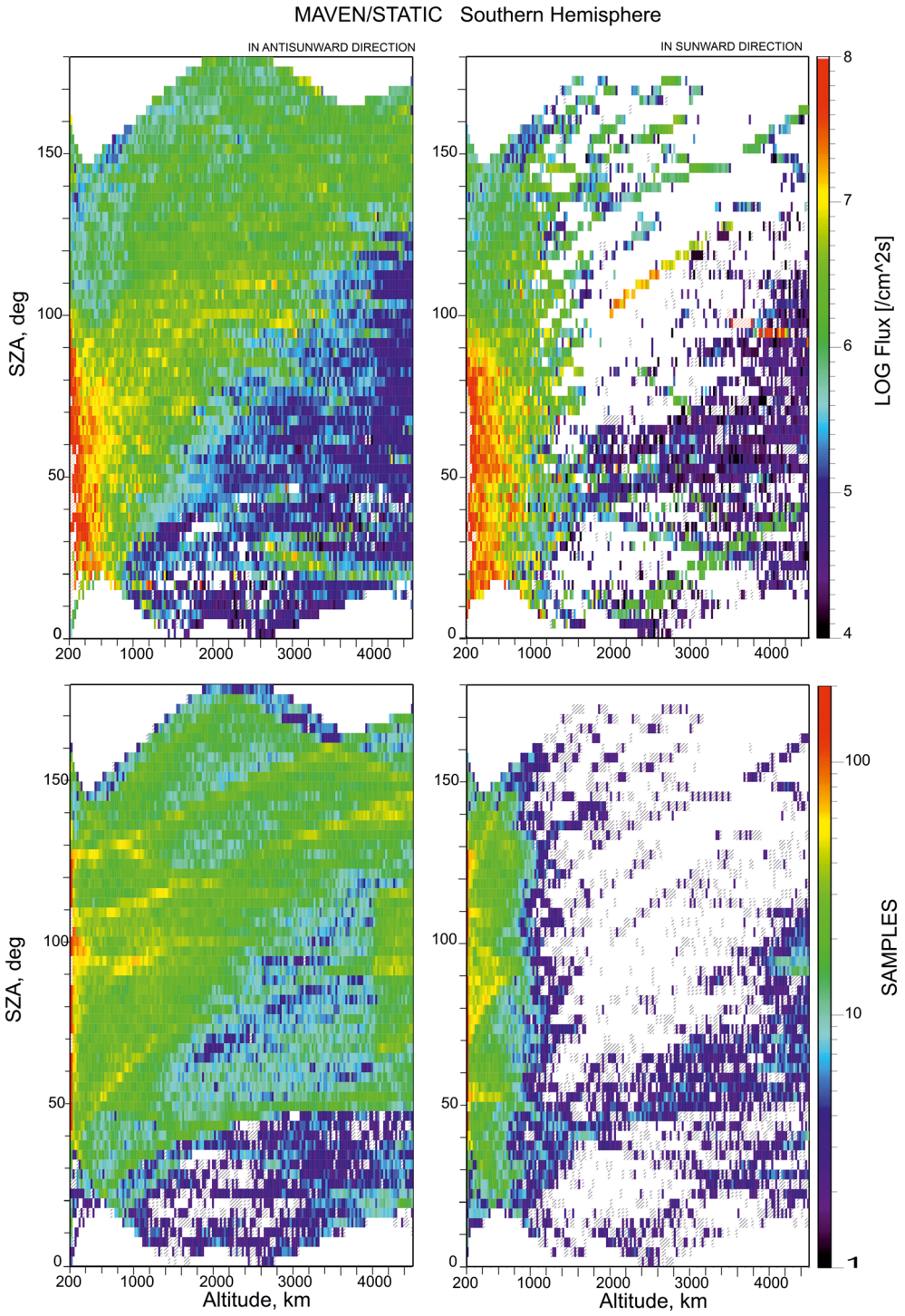

Figure 6. (Upper panels) Maps of the median values of the oxygen ion total fluxes in the southern quadrant with antisunward and sunward component of the ion velocity, respectively. (Lower panels) Number of samples in the each bin.

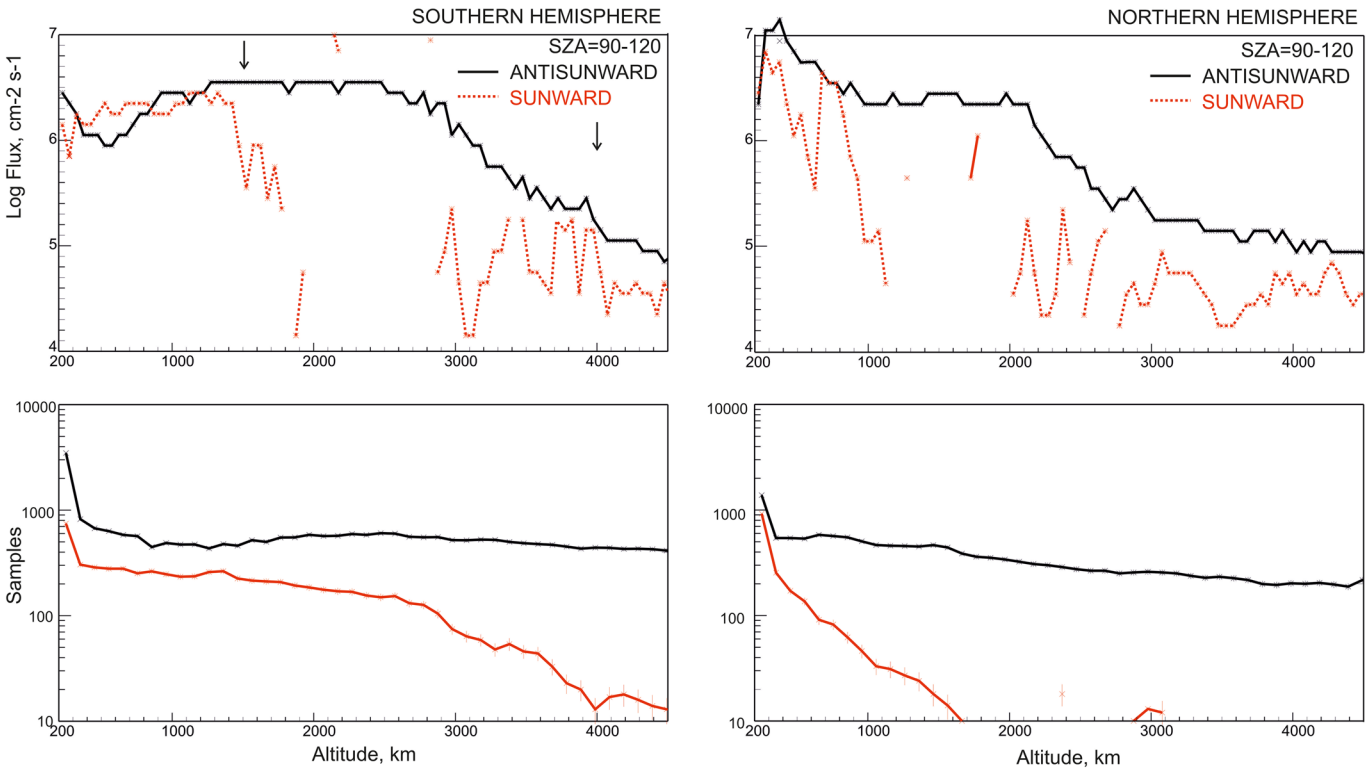

Figure 7. (Upper panels) Altitude profiles of the total ion fluxes with antisunward and sunward component of the ion velocity measured in the southern and the northern quadrants at SZA = 90–120°, respectively. (Lower panels) Corresponding numbers of the measurements in both hemispheres.

we observe the opposite trend, but at higher altitudes the outward fluxes in the southern quadrant prevail that is in a general agreement with the density profiles at these solar zenith angles (Figure 1). The inward ion fluxes are normally lower than the outward fluxes.

Figure 6 (upper panels) compares ion fluxes in the southern quadrant with the negative (antisunward) and positive (sunward) sign of the V_x ion velocity, respectively (in the MSO coordinates the X axis is directed toward the Sun). Note here that it is total flux that combines both either sunward or antisunward component of the V_x velocity. Lower panels show the number of measurements in each bin. We observe that the flow pattern in the dayside southern (SZA $\leq$ 90°) ionosphere at $h \leq$ 700–900 km contains fluxes in both directions that can correspond to cycling motions. Such a motion can significantly decrease the net escape rates.

Figure 7 depicts the values of the total fluxes with the tailward and sunward component of the V_x velocity measured at SZA = 90–120°, and the number of samples in each altitude bin for the northern and the southern quadrants. This interval of solar zenith angles is representative since it covers the area of the transterminator fluxes, which supply the ion population in the tail. In the Southern Hemisphere, at $h \leq$ ~1,000 km the values of fluxes with the opposite sign of the V_x component are comparable. At altitudes of 200–1,200 km, a number of the measurements with return fluxes is about 30–50% of cases with the tailwad streaming ions. So we can use these values estimating the effect of the return fluxes on the total loss. At higher altitudes the return fluxes are rather rare and have lower values. In the northern quadrant we also observe the returning fluxes, but at lower altitudes, their occurrence rate sharply decreases with increase of the height.

Figure 8 presents the measured magnetic field value B_t in the afternoon sector 12–18 hr plotted in the areographic coordinates. Regions occupied by the crustal magnetic field are well seen. Lower panels compare this map with maps of the zonal (azimuthal) ion fluxes in this range of local time and streaming to the nightside and dayside, respectively. In the northern ionosphere the ions are mainly streaming toward the nightside. Return fluxes are almost absent (white areas in the Northern Hemisphere) except for the region at high latitudes where their fluxes are low. In contrast, large ion fluxes flowing toward the dayside are observed in the areas with strong crustal magnetic fields implying cellular convective motions suggested by

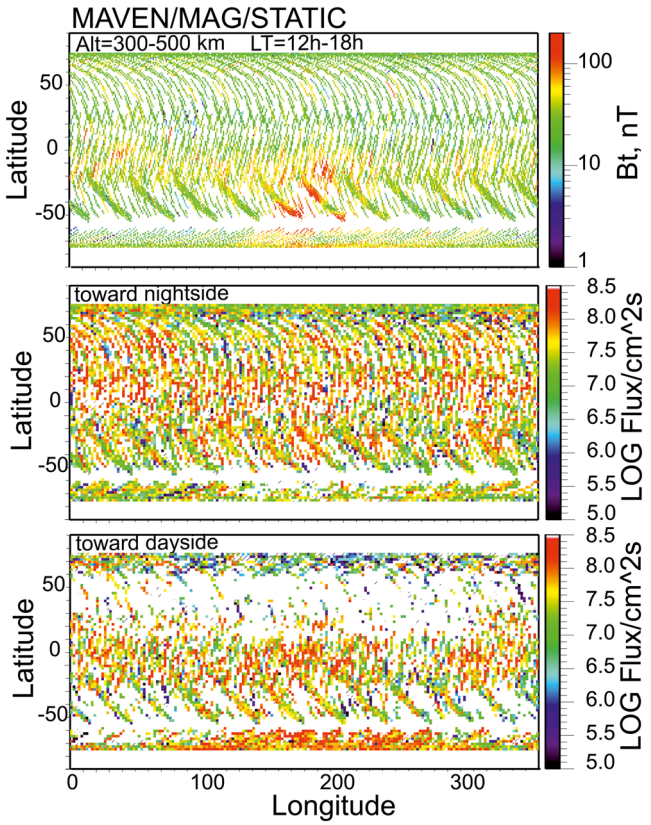

Figure 8. From top to bottom: the magnetic field value plotted in the areographic longitude-latitude coordinates at altitude of 300–500 km in the dayside-dusk sector; zonal ion fluxes with the nightward component of the velocity; zonal ion fluxes with the dayward component of the velocity.

Lundin et al. (2011). Note that white areas in the Southern Hemisphere appear due to the absence of measurements (compare with a map of B_t). Similar features of the flow pattern are observed in the prenoon (6–12 hr) sector.

Figure 9 shows another important effect of the crustal magnetic field. It depicts maps of total ion fluxes with tailward directed component of the V_x velocity for the selected northern and southern quadrants. Lower panels compare the values of the ion fluxes in both hemispheres in different ranges of the solar zenith angle. It is observed that although at low altitudes the fluxes are reduced, at altitudes above ~700, 1,000 and 2,000 km at SZA = 60–90°, 90–120°, and 120–180°, respectively, the antisunward ion fluxes in the Southern Hemisphere begin to prevail. At such altitudes the contribution of the return fluxes is low (Figure 5), and the supply of ions escaping from this area becomes important.

Figure 10 shows the total fluxes of oxygen ions with the tailward directed component of the V_x velocity in the tail at $-3\ R_M < X < -1.3\ R_M$ plotted as a function of the radius $r_{cyl} = \sqrt{(Y^2 + Z^2)}$ in cylindrical coordinates. Black and red curves correspond to the measurements made in the Northern and the Southern Hemispheres, respectively. A reference point (RP) on the Mars surface with the areographic coordinates Lat = −40° and Long = 180° was used to characterize the location of the strong crustal sources of the magnetic field. During the measurements in the tail, the RP was at the dayside (6-12-18 hr). At $r \leq 1\ R_M$ fluxes in the both hemispheres are approximately the same. At $r > 1\ R_M$ fluxes in the Southern Hemisphere predominate. Since the area of the cross section in the tail is proportional to the radius, the excess of ion loss through the Southern Hemisphere reaches ~15% of the total escape rate through the tail.

Asymmetry of ion fluxes in the tail is also controlled by the direction of the motional electric field. Dubinin, Fraenz, et al. (2019) have shown that the ionospheric plasma at the nightside is pushed in the direction opposite to the direction of the motional electric field. As a result, the main channel for ion escape in the tail is shifted toward the Southern Hemisphere at $B_{IMF_y} > 0$. Figure 11 compares these ion fluxes in the tail in

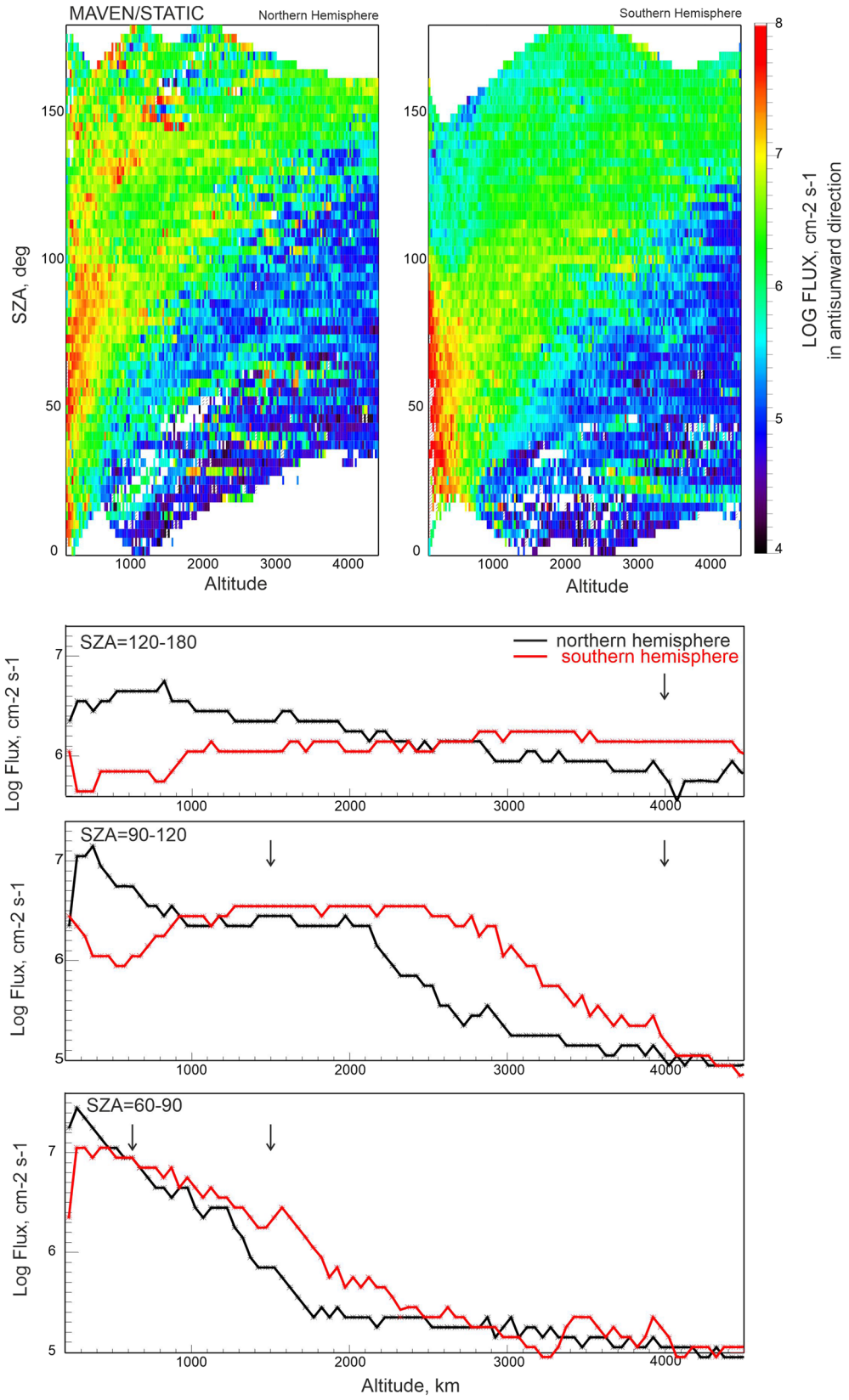

Figure 9. Maps of the median values of the total ion flux of oxygen ions with antisunward component of the ion velocity in the northern and the southern quadrants, respectively. Lower panels show the altitude profiles of these fluxes in several ranges of solar zenith angles.

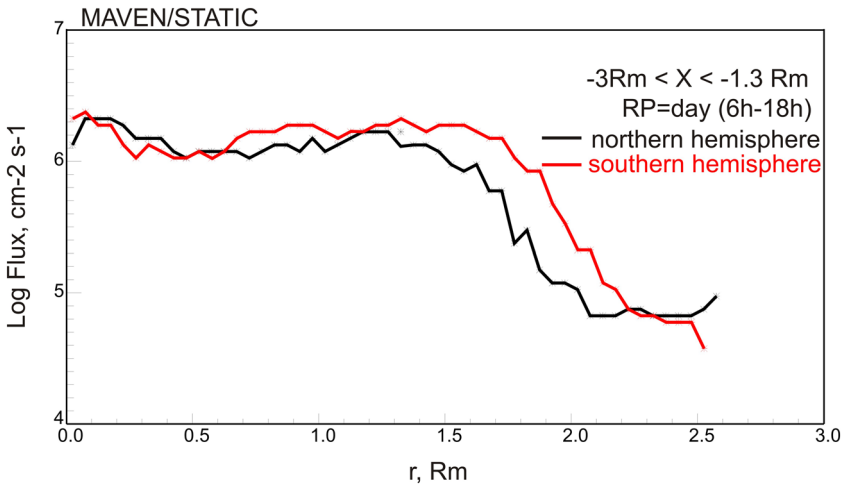

Figure 10. Median values of the oxygen total ion fluxes with the antisunward component of the V_x velocity in the northern and the southern parts of the magnetic tail during the time intervals when the strongest crustal field was at the dayside.

the Northern and the Southern Hemispheres for different signs of the B_{IMF_y} component in the solar wind. It is observed that higher fluxes in the tail in the Southern Hemisphere still remain at $r > 1.5\ R_M$ at $B_{IMF_y} < 0$. At $B_{IMF_y} > 0$ when the effects caused by the crustal magnetic field and by the direction of the motional electric field are in phase, the asymmetry between both hemispheres is enhanced.

Does the averaged statistically estimated ion flux through both hemispheres of the tail depend on the planetary rotation? Figure 12 shows the total ion fluxes through the tail of oxygen ions with tailward directed component of the V_x velocity. The measurements were done in the cross section at $-3\ R_M < X < 1.3\ R_M$ for different position of the reference point related with the strongest crustal magnetic field. We do not observe any noticeable difference in tailward ion fluxes depending on Mars rotation.

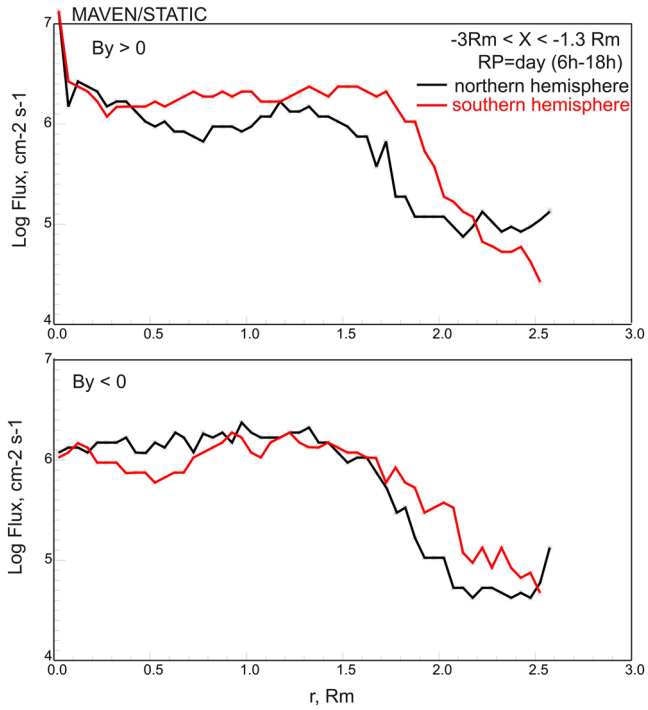

Figure 11. Total ion fluxes with the antisunward component of the V_x velocity in the northern and the southern parts of the magnetic tail measured for the different sign of the B_y component in the solar wind during the time intervals when the strongest crustal field was at the dayside.

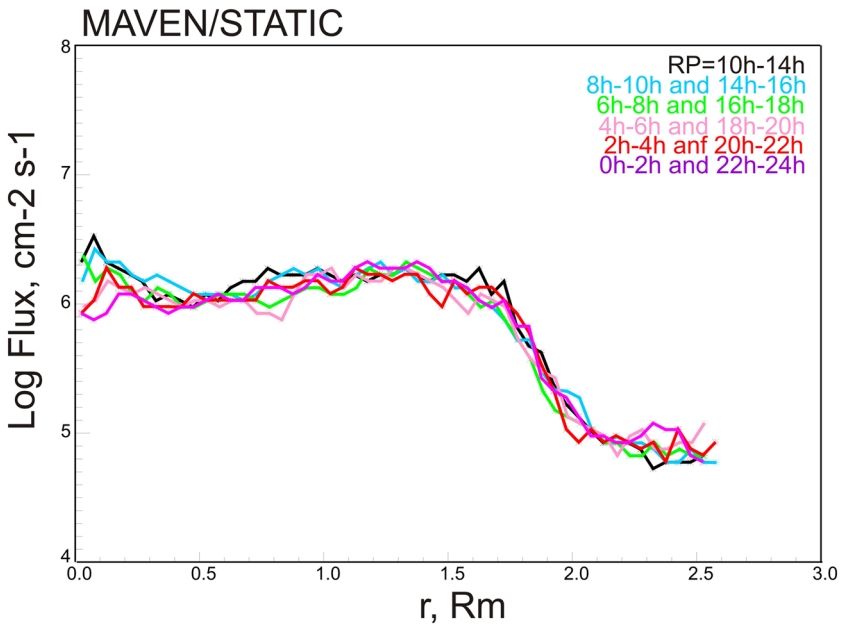

Figure 12. Total ion fluxes with the antisunward component of the V_x velocity in the tail as a function of the rotating crustal magnetic field.

3. Discussion and Conclusions

We have analyzed data obtained by the MAVEN spacecraft to investigate the effect of the crustal magnetic field on ion loss driven by the solar wind interaction with the Martian ionosphere. The crustal magnetic field influences this interaction adding features typical for the planets with a global intrinsic magnetic field. For such planets the escape rate is determined by the areas of the polar cusps and polar caps, and the energy flux transferred to the ionosphere from solar wind (Gunell et al., 2018; Moore & Horwitz, 2007; Strangeway et al., 2010; Tsareva et al., 2020). Mars has no a global intrinsic magnetic field and is partly protected from the solar wind by the magnetic barrier at the dayside formed by the draping interplanetary magnetic field (IMF) lines. Although there is no classical polar cap in the induced magnetosphere of Mars, the total upper dayside ionosphere is permitted by the IMF—the state of the "magnetized" ionosphere by the IMF is typical for Mars—and can be treated as a "polar cap" with ions escaping along the draping field lines to the tail. The mechanism for this process is similar to the one operating in the intrinsic magnetospheres—polar wind driven by the ambipolar electric field (Collinson et al., 2015; Dubinin et al., 2011; Ergun et al., 2016; Ma et al., 2019; Xu et al., 2018). Factors important for the escape in classical polar and auroral winds—the enhanced electron temperature and ion heating by wave power transmitted to the ionosphere—operate at Mars too (Ergun et al., 2016; Fowler et al., 2017). The existence of the tail lobes in the Martian tail filled by low-energy ionospheric ions supports the analogy with the Earth's case (Dubinin et al., 2017).

The crustal magnetic field can significantly modify the field topology by the formation of multiple minimagnetospheres with closed field lines and with minicusps and mini-polar caps with open field lines. Therefore, one can expect an additional protection as well as additional channels for ion losses. At first glance, the question whether the crustal field protects or enhances ion escape has a definite answer. Previous observations (Andrews et al., 2013; Dubinin, Fraenz, et al., 2019; Dubinin et al., 2012, 2016) clearly show that the ionosphere over areas with intense crustal field is less exposed to the ion transport and is much denser and expands to higher altitudes while the ionosphere in the Northern Hemisphere, where the crustal field is much weaker, is more depleted. It was also shown that the ion energization is less efficient in the ionosphere with strong crustal field and correspondingly the escape fluxes of the oxygen ions with $E > 30$ eV are smaller (Fan et al., 2019a).

The data (see Figure 9) presented in this paper show that at lower altitudes (e.g., at $h \leq 600$–700 km at SZA = 60–90° and at $h \leq 1{,}000$ km at SZA = 90–120°), the protection is more efficient in the areas occupied

by the strong crustal field. Ion motions in the ionosphere with the crustal magnetic field at the dayside are significantly suppressed. Moreover, the ion fluxes are often streaming backward creating circular motions as earlier suggested by Lundin et al. (2011). In the Northern Hemisphere the plasma is streaming mainly to the nightside, as one expects for the ideal induced magnetosphere, although at low altitudes, returning fluxes were also measured. Note that the topology of the magnetic field near Mars might be very complex and the regions with closed field lines may appear in the Northern Hemisphere too (Xu et al., 2017).

On the other hand, at higher altitudes the ion fluxes above the regions with strong crustal fields are larger than the corresponding fluxes in the Northern Hemisphere where the crustal fields are weak. This happens because the ionosphere at the dayside over the areas with strong crustal field is thicker and the ion densities are larger. As a result of the larger area of the ionospheric cross section being exposed to the solar wind, the ion loss rate increases. A strong positive correlation between the cross-section area and ion loss was also observed in MHD simulations (Fang et al., 2015). Thus, a shielding mechanism operates at lower altitudes while the effect of the ionosphere thickness becomes more important with increase of altitude. Since both effects operate in antiphase, it is not surprising that no statistically significant difference in the escape rates from the Northern and the Southern Hemispheres was observed in earlier studies (see, e.g., Lundin et al., 2011; Nilsson et al., 2011; Ramstad et al., 2016). Our analysis of the measurements in the tail shows that the effect of the ionospheric cross-section area being exposed to the solar wind prevails and the fluxes observed in the Southern Hemisphere occur higher. The excess in the total escape rate through the Southern Hemisphere is about 15%.

Observations by Dubinin, Modolo, et al. (2019) and Inui et al. (2019) have shown that an asymmetry of escape fluxes between both hemispheres may also be related with the sign of the B_y component of the IMF. This effect is related to features of the induced magnetosphere—the ionospheric plasma at the nightside is pushed in the direction opposite to the direction of the motional electric field in the solar wind. As a result, the main channel for ion escape in the tail is shifted toward the Southern Hemisphere at $B_{IMF_y} > 0$ enhancing the effect of the crustal magnetic field. We have shown in this paper that even for $B_{IMF_y} < 0$ effects of the increased area of the ionosphere cross section being exposed to the solar wind are still noticeable although are weaker.

We do not observe a noticeable effect related with the rotation of the crust field while considering the averaged fluxes in the both hemispheric tail lobes. It is worth noting that in our paper we have analyzed the statistically averaged ion fluxes for 4 years and therefore seasonal effects, effects related due to the large eccentricity of Mars orbit as well as variations in solar wind and solar EUV flux, may reduce modulations in escape rates related to the rotation of the crustal field.

In conclusion, the crustal magnetic field at Mars weakens the ion motions in the ionosphere and causes the appearance of returning fluxes. However, due to the higher ion number densities in the ionosphere over the crustal field sources, their net transport to the tail remains crucial. Another important effect of the crustal magnetic field is related with the ionospheric expansion to higher altitudes and the increase of the cross-section area exposed to the solar wind. With increase of altitude the ion fluxes from the ionosphere over the areas with strong crustal magnetic field begin to overcome the corresponding fluxes from the ionosphere with a weak field. Interplay of these competing processes leads to excess of ion losses through the southern part of the magnetic tail (~15%). The strength of asymmetry of the ion fluxes in the tail between both hemispheres is also sensitive to the sign of the cross-flow component of the IMF.

Data Availability Statement

MAVEN data are publicly available through the Planetary Data System (https://pds-ppi.igpp.ucla.edu/mission/MAVEN).

Acknowledgments
The MAVEN project is supported by NASA through the Mars Exploration Program. Authors E. D. and M. P. wish to acknowledge support from DFG for supporting this work by Grant PA 525/24-1. Authors E. D. and M. F. wish to acknowledge support from DLR by Grant 50QM1703. O. V. and L. Z. wish to acknowledge support from the Russian Science Foundation by Grant 20-42-04418.

References

Acuna, M. H., Connerney, J. E. P., Ness, N. F., Lin, R. P., Mitchell, D., Carlson, C. W., et al. (1999). Global distribution of crustal magnetism discovered by Mars Global Surveyor MAG/ER experiment. *Science*, *284*, 790–793. https://doi.org/10.1126/science.284.5415.790

Andrews, D. J., Opgenoorth, H. J., Edberg, N. J. T., André, M., Fränz, M., Dubinin, E., et al. (2013). Determination of local plasma densities with the MARSIS radar: Asymmetries in the high altitude Martian ionosphere. *Journal of Geophysical Research: Space Physics*, *118*, 6228–6242. https://doi.org/10.1002/jgra.50593

Barabash, S., Fedorov, A., & Lundin, R. (2007). Sauvaud, J. A. *Martian atmospheric erosion rates. Science*, *315*, 501–503. https://doi.org/10.1126/science.1134358

Brain, D. A., Baker, A. H., Briggs, J., Eastwood, J. P., Halekas, J. S., & Phan, T.-D. (2010). Episodic detachment of Martian crustal magnetic fields leading to bulk atmospheric plasma escape. *Geophysical Research Letters*, *37*, L14108. https://doi.org/10.1029/2010GL043916

Brain, D. A., McFadden, J. P., Halekas, J. S., Connerney, J. E. P., Bougher, S. W., Curry, S., et al. (2015). The spatial distribution of planetary ion fluxes near mars observed by MAVEN. *Geophysical Research Letters*, *42*, 9142–9148. https://doi.org/10.1002/2015GL065293

Brecht, S. H., & Ledvina, S. A. (2014). The role of the Martian crustal magnetic fields in controlling ionospheric loss. *Geophysical Research Letters*, *41*, 5340–5346. https://doi.org/10.1002/2014GL060841

Collinson, G., Mitchell, D., Glocer, A., Grebowsky, J., Peterson, W. K., Connerney, J., et al. (2015). Electric Mars: The first direct measurement of an upper limit for the Martian "polar wind" electric potential. *Geophysical Research Letters*, *42*, 9128–9134. https://doi.org/10.1002/2015GL065084

Connerney, J. E. P., Espley, J., Lawton, P., Murphy, S., Odom, J., Oliversen, R., & Sheppard, D. (2015). The MAVEN magnetic field investigation. *Space Science Reviews*, *195*(1–4), 257–291. https://doi.org/10.1007/s11214-015-0169-4

Dubinin, E., Fraenz, M., Andrews, D., & Morgan, D. (2016). Martian ionosphere observed by Mars Express: 1. Influence of the crustal magnetic fields. *Planetary and Space Science*, *124*, 62–75. https://doi.org/10.1016/j.pss.2016.02.004

Dubinin, E., Fraenz, M., Fedorov, A., Lundin, R., Edberg, N., Duru, F., & Vaisberg, O. (2011). Ion energization and escape on Mars and Venus. *Space Science Reviews*, *162*, 173–211. https://doi.org/10.1007/978-1-4614-3290-6-6

Dubinin, E., Fraenz, M., Pätzold, M., McFadden, J., Halekas, J. S., DiBraccio, G. A., et al. (2017). The effect of solar wind variations on the escape of oxygen ions from mars through different channels: MAVEN observations. *Journal of Geophysical Research: Space Physics*, *122*, 11,285–11,301. https://doi.org/10.1002/2017JA024741

Dubinin, E., Fraenz, M., Pätzold, M., Woch, J., McFadden, J., Halekas, J. S., et al. (2019). Expansion and shrinking of the martian topside ionosphere. *Journal of Geophysical Research: Space Physics*, *124*, 9725–9738. https://doi.org/10.1029/2019JA027077

Dubinin, E., Fraenz, M., Woch, J., Barabash, S., Lundin, R., Winningham, J. D., et al. (2006). Plasma Morphology at Mars: ASPERA-3 Observations. *Space Science Reviews*, *126*, 209–238. https://doi.org/10.1007/s11214-006-9039-4

Dubinin, E., Fraenz, M., Woch, J., Modolo, R., Chanteur, G., Duru, F., et al. (2012). Upper atmosphere of mars is not axially symmetrical. *Earth, Planets and Space*, *64*, 113–120. https://doi.org/10.5047/eps.2011.05.022

Dubinin, E., Modolo, R., Fraenz, M., Pätzold, M., Woch, J., Chai, L., et al. (2019). The induced magnetosphere of Mars: Asymmetrical topology of the magnetic field lines. *Geophysical Research Letters*, *46*, 12,722–12,730. https://doi.org/10.1029/2019GL084387

Egan, H., Jarvinen, R., Ma, Y., & Brain, D. (2019). Planetary magnetic field control of ion escape from weakly magnetized planets. *Monthly Notices of the Royal Astronomical Society*, *488*(2), 2108–2120. https://doi.org/10.1093/mnras/stz1819

Ergun, R. E., Andersson, L., Fowler, C. M., Woodson, A., Weber, T., Delory, G., et al. (2016). Enhanced O_2^+ loss at mars due to an ambipolar electric field from electron heating. *Journal of Geophysical Research: Space Physics*, *121*, 4668–4678. https://doi.org/10.1002/2016JA022349

Fan, K., Fraenz, M., Wei, Y., Han, Q., Dubinin, E., Cui, J., et al. (2019). Reduced atmospheric ion escape above martian crustal magnetic fields. *Geophysical Research Letters*, *46*, 11,764–11,772. https://doi.org/10.1029/2019GL084729

Fang, X., Ma, Y., Brain, D., Dong, Y., & Lillis, R. (2015). Control of Mars global atmospheric loss by the continuous rotation of the crustal magnetic field: A time-dependent MHD study. *Journal Geophysical Research: Space Physics*, *120*, 10,926–10,944. https://doi.org/10.1002/2015JA021605

Fowler, C. M., Ergun, R. E., Andersson, L., Peterson, W. K., Hara, T., Mcfadden, J., et al. (2017). Ion heating in the Martian ionosphere. *Journal of Geophysical Research: Space Physics*, *122*, 10,612–10,625. https://doi.org/10.1002/2017JA024578

Fraenz, M., Dubinin, E., Andrews, D., Barabash, S., Nilsson, H., & Fedorov, A. (2015). Cold ion escape from the martian ionosphere. *Planetary and Space Science*, *119*(15), 92–102. https://doi.org/10.1016/j.pss.2015.07.012

Fraenz, M., Dubinin, E., Nielsen, E., Woch, J., Barabash, S., Lundin, R., & Fedorov, A. (2010). Transterminator ion flow in the Martian ionosphere. *Planetary and Space Science*, *58*, 1442–1454. https://doi.org/10.1016/j.pss.2010.06.009

Gunell, H., Maggiolo, R., Nilsson, H., Wieser, G. S., Slapak, R., Lindkvist, J., et al. (2018). Lindkvist Why an intrinsic magnetic field does not protect a planet against atmospheric escape. *Astronomy and Astrophysics*, *614*(L3), 8. https://doi.org/10.1051/0004-6361/201832934

Harnett, E. M. (2009). High-resolution multifluid simulations of flux ropes in the martian magnetosphere. *Journal of Geophysical Research*, *114*, A01208. https://doi.org/10.1029/2008JA013648

Inui, S., Seki, K., Sakai, S., Brain, D. A., Hara, T., McFadden, J. P., et al. (2019). Statistical study of heavy ion outflows from mars observed in the Martian induced magnetotail by MAVEN. *Journal Geophysical Research: Space Physics*, *124*, 5482–5497. https://doi.org/10.1029/2018JA026452

Jakosky, B. M., Lin, R. P., Grebowsky, J. M., Luhmann, J. G., Mitchell, D. F., Beutelschies, G., et al. (2015). The Mars Atmosphere and Volatile Evolution (MAVEN) mission. *Space Science Reviews*, *195*(1–4), 3–48. https://doi.org/10.1007/s11214-015-0139-x

Lundin, R., Barabash, S., Yamauchi, M., Nilsson, H., & Brain, D. (2011). On the relation between plasma escape and the Martian crustal magnetic field. *Geophysical Research Letters*, *38*, L02102. https://doi.org/10.1029/2010GL046019

Lundin, R., Zakharov, A., Pellinen, R., Borg, H., Hultqvist, B., Pissarenko, N., et al. (1989). First measurements of the ionospheric plasma escape from Mars. *Nature*, *341*, 609–612. https://doi.org/10.1038/341609a0

Ma, Y. J., Dong, C. F., Toth, G., van der Holst, B., Nagy, A. F., Russell, C. T., et al. (2019). Importance of ambipolar electric field in driving ion loss from Mars: Results from a multifluid MHD model with the electron pressure equation included. *Journal of Geophysical Research: Space Physics*, *124*, 9040–9057. https://doi.org/10.1029/2019JA027091

Ma, Y., Fang, X., Russell, C. T., Nagy, A. F., Toth, G., Luhmann, J. G., et al. (2014). Effects of crustal field rotation on the solar wind plasma interaction with Mars. *Geophysical Research Letters*, *41*, 6563–6569. https://doi.org/10.1002/2014GL060785

Ma, Y., Nagy, A. F., Hansen, K. C., DeZeeuw, D. L., Gombosi, T. I., & Powell, K. G. (2002). Three-dimensional multispecies MHD studies of the solar wind interaction with Mars in the presence of crustal fields. *Journal of Geophysical Research*, *107*(A10), 1282. https://doi.org/10.1029/2002JA009293

McFadden, J. P., Kortmann, O., Curtis, D., Dalton, G., Johnson, G., Abiad, R., et al. (2015). MAVEN SupraThermal and Thermal Ion Compostion (STATIC) instrument. *Space Science Reviews*, *195*, 199–256. https://doi.org/10.1007/s11214-015-175-6

Moore, T. E., & Horwitz, J. L. (2007). Stellar ablation of planetary atmospheres. *Reviews of Geophysics*, *45*, RG3002. https://doi.org/10.1029/2005RG000194

Nilsson, H., Edberg, N., Stenberg, G., Barabash, S., Futaana, Y., Holmstrom, M., et al. (2011). Total heavy ion escape from Mars and influence from solar wind conditions and crustal magnetic fields. *Icarus*, *215*, 475–484. https://doi.org/10.1016/j.icarus.2011.08.003

Ramstad, R., Barabash, S., Futaana, Y., Nilsson, H., & Holmstrom M. (2016). Effects of the crustal magnetic fields on the Martian atmospheric ion escape rate. *Geophysical Research Letters*, *43*, 10,574–10,579. https://doi.org/10.1002/2016GL070135

Ramstad, R., Barabash, S., Futaana, Y., Nilsson, H., & Holmstrom M. (2017). Global Mars-solar wind coupling and ion escape. *Journal of Geophysics Research: Space Physics*, *122*, 8051–8062. https://doi.org/10.1002/2017JA024306

Sakai, S., Seki, K., Terada, N., Shinagawa, H., Tanaka, T., & Ebihara, Y. (2018). Effects of a weak intrinsic magnetic field on atmospheric escape from Mars. *Geophysical Research Letters*, *45*, 9336–9343. https://doi.org/10.1029/2018GL079972

Strangeway, R. J., Russell, C. T., Luhmann, J. G., Moore, T. E., Foster, J. C., Barabash, S. V., & Nilsson, H. (2010). Does a planetary-scale magnetic field enhance or inhibit ionospheric plasma outflows? AGU Fall Meeting Abstracts.

Tsareva, O. O., Dubinin, E., Malova, H., Popov, V., & Zelenyi L. (2020). Atmospheric escape from the Earth during geomagnetic reversal. *Annales Geophysics*, *62*, PA 222. https://doi.org/10.4401/ag8354

Xu, S., Mitchell, D., Luhmann, J., Ma, Y., Fang, X., Harada, Y., et al. (2017). High-altitude closed magnetic loops at mars observed by MAVEN. *Geophysical Research Letters*, *44*, 11,229–11,238. https://doi.org/10.1002/2017GL075831

Xu, S., Mitchell, D. L., McFadden, J. P., Collinson, G., Harada, Y., Lillis, R., et al. (2018). Field-aligned potentials at Mars from MAVEN observations. *Geophysical Research Letters*, *45*, 10,119–10,127. https://doi.org/10.1029/2018GL080136